Journal of Materials Science: Materials in Electronics (2019) 30:6537–6543
https://doi.org/10.1007/s10854-019-00959-0

Investigation on the electromagnetic and broadband microwave absorption properties of Ti_3C_2 Mxene/flaky carbonyl iron composites

Shuoqing Yan[1] · Can Cao[2] · Jun He[2] · Longhui He[2] · Zewen Qu[2]

Received: 24 November 2018 / Accepted: 16 February 2019 / Published online: 26 February 2019

Abstract
A high-performance microwave absorption material is highly demanded. Herein, the laminated Ti_3C_2 Mxene was synthesised via HF etching process, and the flaky carbonyl iron (FCI) particles were prepared by high-energy ball milling. The hybrid Ti_3C_2/FCI powders with different mass ratios were fabricated by ultrasonic mixing method. Electromagnetic and microwave absorption properties of the single layer Ti_3C_2/FCI coatings were investigated in 2–18 GHz. A broadened microwave absorption property can be realized by optimizing the Ti_3C_2 and FCI content. Especially, the coating with 20 wt% Ti_3C_2 and 40 wt% FCI loading presents the measured absorption bandwidth (RL < − 10 dB) of 8.16 GHz with the thickness of 1.0 mm. The remarkable microwave absorbing performance was attributed to the good impedance matching and moderate attenuation ability. These results indicate that the Ti_3C_2/FCI composites have great potential to be a broadband microwave absorbent.

1 Introduction

The rapid development of microwave electronic devices leads to increasingly electromagnetic (EM) interference problems. Microwave absorption materials can eliminate adverse electromagnetic energy, and have attracted extensive interests [1–3]. Broadband microwave absorption is critical for a microwave absorption (MA) material since microwave electronic devices work in a wide frequency range. To achieve this goal, the key problem focus on exploration of materials exhibiting multiple EM waves loss mechanism and good impedance matching property [4–6]. Considerable researches have shown that the combination of dielectric absorber and magnetic absorber is a good choice to solve this problem [7–10].

Two dimensional (2D) materials with laminated, porous and 3D-network structures are proved to be high-performance microwave absorbers. Specially, newly emerged 2D material labeled as Ti_3C_2 MXene is kinds of dielectric-type absorption material with potential broad absorption bandwidth. Qing et al. [11] successfully synthesized Ti_3C_2 MXene nanosheets and absorption bandwidth of 5.6 GHz was obtained with a thickness of 1.4 mm. Feng et al. [12] reported that the Ti_3C_2 MXene nanosheets exhibited an effective absorbing bandwidth of 6.8 GHz at 2 mm. The microwave absorption property of the Ti_3C_2 MXene is mainly attributed to its 2D laminated morphology, active surface functional groups, native defect and extraordinary electric conductivity [11, 12]. Nevertheless, a relatively high permittivity for the Ti_3C_2 MXene is unfavorable to impedance matching and dissipation of EM waves. Mixing a magnetic absorber with Ti_3C_2 MXene is necessary. In previous reports, the Ti_3C_2 MXene/$Ni_{0.5}Zn_{0.5}Fe_2O_4$ [13] and Ti_3C_2 MXene/Fe_3O_4 [14] have been studied for enhanced microwave absorption. However, the complex fabrication process of these composites restricted their practical application. Also, the large-scale synthesis of these composites remains a significant challenge. Compared with $Ni_{0.5}Zn_{0.5}Fe_2O_4$ and Fe_3O_4, the carbonyl iron (CI) particles are so far considered as the most attractive magnetic absorbents, with the advantages of high magnetic loss in GHz range, large-scale fabrication and low cost [15, 16]. Furthermore, flaky carbonyl iron (FCI) have larger values of permeability since its Snoke's limit is located at a higher frequency [5, 17–19]. Besides, broad absorption bandwidth has been reported in a variety of dielectric materials/FCI composites [3, 20, 21]. In view of this, we focus on the combined dielectric loss of the Ti_3C_2 MXene and magnetic loss of the FCI to firstly develop

✉ Can Cao
caocan@csu.edu.cn

[1] College of Science, Hunan Institute of Engineering, Xiangtan 411104, China

[2] School of Physics and Electronics, Central South University, Changsha 410083, China

single-layer microwave absorbing coating with broadband microwave absorption.

2 Experimental and characterizations

The Ti_3C_2 MXenes were synthesized via HF etching process [11, 12]. The commercial Ti_3SiC_2 powders (Forsman Scientific Co. Ltd. Beijing) were chosen as a raw material. Initially, 10 g Ti_3SiC_2 was added into HF solution (40 wt%) of 100 mL. The acidic solution was magnetically stirred for 72 h at room temperature to extract Si from the Ti_3SiC_2 particles. Then the obtained solution were washed with deionized water several times to remove the residual HF until the pH of the solution was about 7. Finally, the mixture was centrifuged to obtain black powders, and the resulting powders was dried at 80 °C for 1 h to obtained the Ti_3C_2 MXenes.

The FCI particles were prepared by high energy ball-milling reported in our previous study [21]. Raw spherical carbonyl iron (SCI) powders were purchased from Jiangsu Tianyi Ultrafne metal powder Co. Ltd.. Typically, 2 kg SCI powders, 30 kg bearing steel ball (Φ3 mm) and 3 kg absolute ethanol were milled in vertical ball mill machine with 900 rpm for 6 h. The as-milled mixture was filtered and dried under vacuum at 60 °C for 5 h to obtain the FCI particles.

The hybrid powders were fabricated by blending Ti_3C_2 MXenes with the milled FCI thoroughly in the ultrasonic bath. The mass ratios of Ti_3C_2 MXenes to FCI were 1:0, 2:1, 1:1, 1:2, and 0:1, respectively. Following, the hybrid absorbers were mechanically dispersed in epoxy resin to form a homogeneous dispersion. An aluminum plate of dimensions 180 mm × 180 mm × 5 mm was used as a substrate. The homogenous mixture was sprayed on the aluminum plate layer by layer to prepare the absorbing coating [22]. The actually achieved mass fraction of hybrid absorbers in the absorbing coating were 60 wt%. The coaxial cylinder specimens with outer diameter of 7.00 mm and inner diameter of 3.04 mm were also made of the mixture of as-prepared hybrid absorbers (60 wt%) and epoxy resin.

X-ray diffraction (XRD) characterization was acquired on Rigaku Ultima IV diffractometer (Cu Kα radiation, $\lambda = 1.5406$ Å). The morphology and composition of the samples were examined by FEI Nova NanoSEM field-emission scanning electron microscope. The magnetic properties was obtained on a vibration sample magnetometer (VSM, Lake-Shore 7307). The relative complex permittivity (ε_r) and permeability (μ_r) were measured by a vector network analyzer (Agilent N5230A) in the frequency range of 2–18 GHz. The RL values of coating were measured by the arched reflecting method that was detailed described in Ref. [23].

3 Results and discussion

The morphology and microstructure of Ti_3SiC_2 before and after the HF treatment were investigated by SEM images and the results are shown in Fig. 1a, b. After etching by HF, laminated structure of Ti_3C_2 MXene can be observed,

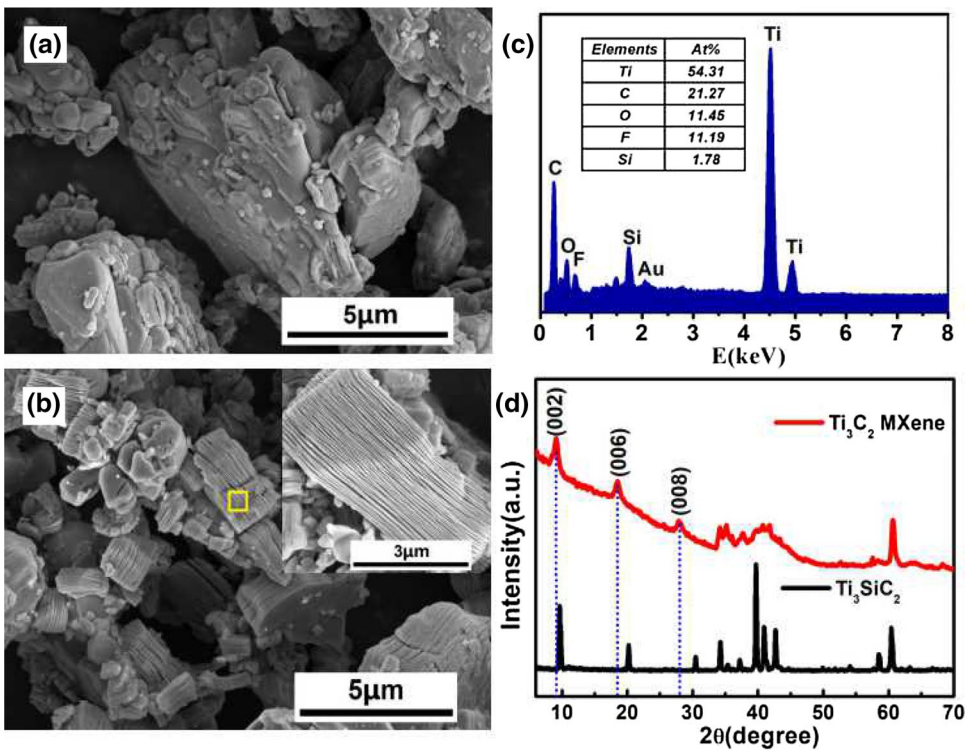

Fig. 1 The morphology of **a** Ti_3SiC_2 and **b** Ti_3C_2 MXene; **c** EDS spectrum and **d** XRD patterns of the Ti_3C_2 MXene

suggesting the successful exfoliation. Besides, the investigated EDS [see in Fig. 1c] exhibit that the as-prepared Ti_3C_2 MXene is mainly composed of Ti and C, indicating the elimination of Si. Additional O and F result from etching by HF. The typical XRD patterns of the Ti_3SiC_2 and Ti_3C_2 samples are shown in Fig. 1d. Apparently, the observed peaks of Ti_3C_2 MXene are agreement with the previous study [11, 12], implying the successful synthesis of Ti_3C_2 MXene by HF etching. In addition, the XRD peaks of the as-prepared Ti_3C_2 MXene are broadened and shifted to lower angles (especially for (002), (006) and (008) peaks) compared with those of raw material Ti_3SiC_2 powders. The unique morphology and microstructure of Ti_3C_2 MXene are beneficial to the improvement of microwave absorption capability.

Figure 2a, b show the morphology of raw CI and FCI particles, respectively. The particles of raw CI are spherical shape with a mean size of 3.5 μm. The achieved thin flake-like carbonyl iron particles with the ball milling were presented in Fig. 2b. No spherical particles can be found. The diameters of FCI were mostly in the range of 6–15 μm. The identified flake morphology are favorable for the enhancement of complex permeability [17, 18]. Figure 2c shows the typical XRD patterns of FCI powders. Only three characteristic diffraction peaks at $2\theta = 44.5°$, 64.9° and 82.2° were observed. They are respectively associated with the (110), (200) and (211) of cubic structure α-Fe (identified by JCPDS 06-0696) [15, 16]. The observed broad XRD peaks indicate larger particle size for FCI. Magnetic hysteresis loops of the FCI sample is displayed in Fig. 2d. The saturation magnetization (M_s) and coercivity (H_c) are 195.46 emu/g, 20.52 Oe, suggesting excellent ferromagnetism for the FCI powders. The larger M_s can effectively increase the permeability of the composites by increasing the FCI powders conten.

Figure 3 displays the real part (ε') and imaginary part (ε'') of permittivity for the Ti_3C_2 MXene/FCI composites with different mass ratios in 2–18 GHz. It is obvious that both ε' and ε'' rise across the whole frequency range with the mass ratio of Ti_3C_2 increasing. ε' and ε'' for the sole FCI-filled specimen are 13.68 and 0.72 at 2 GHz, respectively. This low complex permittivity indicates weaken dielectric loss. When only the Ti_3C_2 MXene loading, ε' and ε'' increase to 44.61 and 20.39, suggesting a larger dielectric loss. In addition, the ε' and ε'' curves show typical nonlinear resonant characteristics. Such phenomena can be attributed to various polarizations. Generally, the ε' mainly arises from the dipole polarization and interfacial polarization in GHz frequency range [24, 25]. In compared with the FCI particles, a large quantity of lattice defects and functional groups were created in Ti_3C_2 MXene synthesis processing, resulting in more electric dipoles and dipole polarization under an alternating electrical. Besides, the SEM image of Ti_3C_2 MXene shows a laminated morphology and large surface area. When

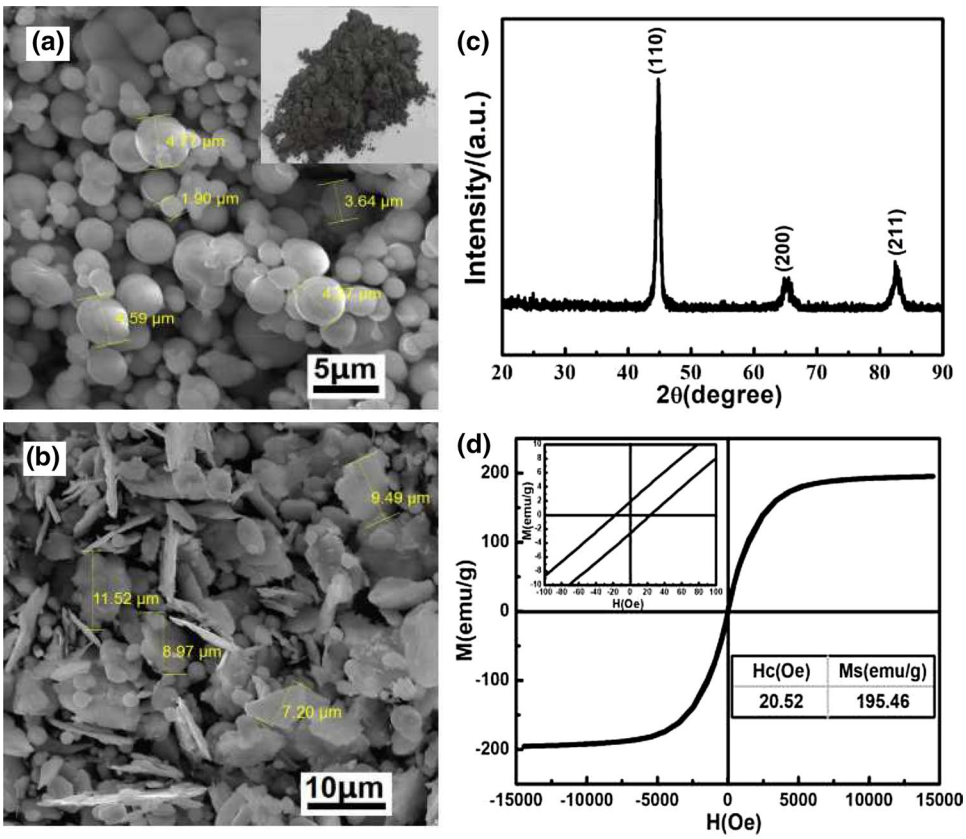

Fig. 2 SEM image of **a** raw CI particles and **b** milled FCI particles; **c** XRD patterns and **d** VSM of the milled FCI powder

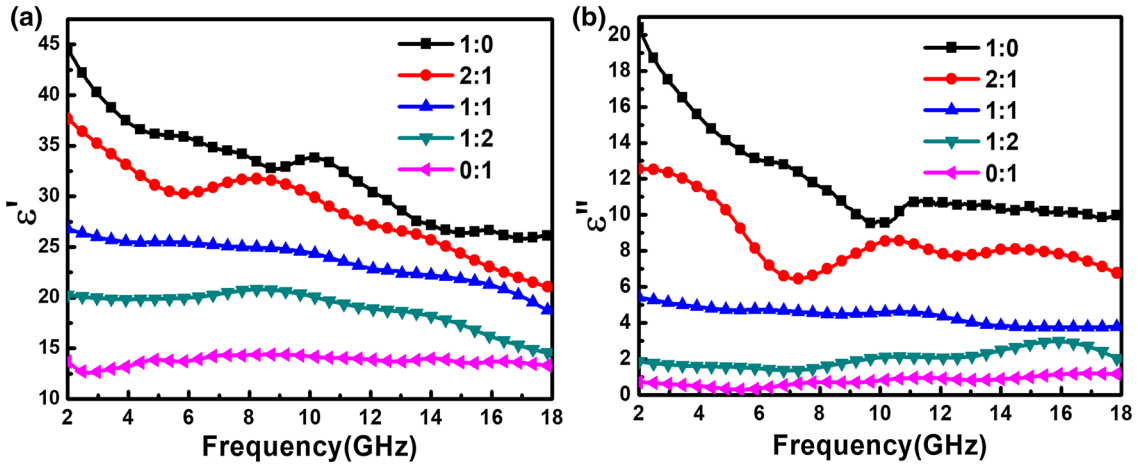

Fig. 3 Frequency dependence of complex permittivity for the Ti_3C_2 MXene/FCI composites with different mass ratios

the laminated Ti_3C_2 MXenes were embedded in insulated matrix, abundant interfaces can be found between Ti_3C_2 MXene and insulated matrix. Those abundant interfaces finally inducing stronger interface polarization under the alternating electrical field. On the other hand, ε'' is known as an expression of the dielectric loss ability of materials. The value of ε'' is related to the relaxation polarization loss and the electric conductance loss [26, 27]. The Ti_3C_2 MXene is highly electrical conductive absorber in compared with the FCI. Increased mass ratio of Ti_3C_2 makes a contribution to forming the conductive network and enhanced polarization ability, which results in the enhancement of ε''.

The real part (μ') and imaginary part (μ'') of permeability for the Ti_3C_2 MXene/FCI composites with various mass ratios in 2–18 GHz are illustrated in Fig. 4. Apparently, both μ' and μ'' increase with the FCI content increasing. As the Ti_3C_2 MXene/FCI mass ratios change from 1:0 to 0:1, μ' increases from 1.05 to 3.24, and μ'' raise from 0.03 to 0.95. Specially, the μ' and μ'' of the Ti_3C_2 MXene sample nearly 1 and 0, indicating inexistence of magnetic loss. For the individual FCI specimen, in contrast, the maximum values of μ' and μ'' are 3.24 and 1.23, respectively. Moreover, the μ'' curves of all FCI-filled samples exhibit broad peaks, which contributes to broaden absorption bandwidth and strengthen absorptivity of electromagnetic waves. This characteristic can be attributed to the high ferromagnetic resonant frequency for flaky FCI particles. The similar result was also reported in previous work [17, 18]. Therefore, the magnetic characteristics of the hybrid Ti_3C_2 MXene/FCI powders are mainly dominated by those of FCI, in view of the fact that Ti_3C_2 MXene is a nonmagnetic material. As a result, the above results indicate that the electromagnetic properties of the coating can be tailored via changing the mass ratio of the filled absorber.

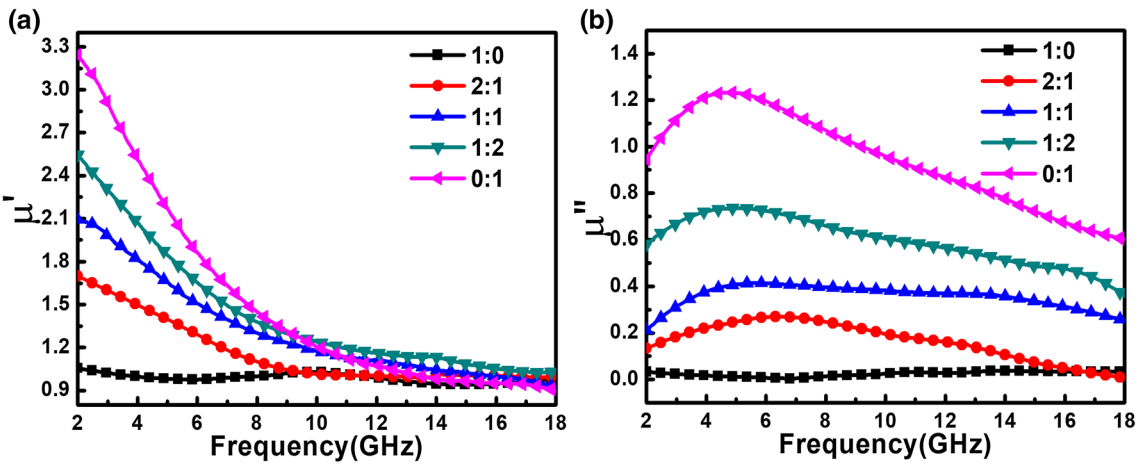

Fig. 4 Frequency dependence of complex permeability for the Ti_3C_2 MXene/FCI composites with different mass ratios

To further investigate the influence of Ti_3C_2 MXene/FCI ratio on the EM wave absorption properties, The absorbing coatings based on different mass ratios of Ti_3C_2 MXene/FCI [see in Fig. 5(b)] were prepared with thickness of 1.0 mm. The RL values in 2–18 GHz were measured and shown in Fig. 5a. The most important and interesting observation is that the RL is found to depend sensitively on the mass ratios of the Ti_3C_2 MXene/FCI. Relative to all coatings, the coating with mass ratios of 1:2 loading displays optimized microwave absorbing capability. The effective absorption bandwidth (RL < − 10 dB) of 8.16 GHz was realized. As shown in Fig. 5c, the SEM image of the coating with mass ratios of 1:2 loading shows the uniform dispersion of two absorbent in epoxy resin. The excellent microwave absorption property is attributed to the coexistence of dielectric loss and magnetic loss. Detailed RL values of the Ti_3C_2 MXene/FCI composites and a comparison of other representative FCI-based and Ti_3C_2 MXene-based composites reported in recent literatures were summarized and listed in Table 1. Obviously, by combing the properties of dielectric absorber and magnetic absorber has been used to improve the absorption efficiency of the absorber. The Ti_3C_2 MXene/FCI composite with appropriate mass ratio prepared in this work exhibits superior performance at a broad absorption bandwidth and thin thickness. Those results indicate the promising perspective of the Ti_3C_2 MXene/FCI absorber in the development of broadband microwave absorbing coatings.

Microwave absorption materials with wide absorption bandwidth require stronger EM wave dissipation ability as well as excellent EM impedance matching property. The attenuation constant (γ) is usually applied to evaluate the EM dissipation ability. The γ can be illustrated as follows [31]:

$$\gamma = \frac{2\pi f}{c}\sqrt{(\mu''\varepsilon'' - \mu'\varepsilon') + \sqrt{(\mu''\varepsilon'' - \mu'\varepsilon')^2 + (\mu'\varepsilon'' + \mu''\varepsilon')^2}} \quad (1)$$

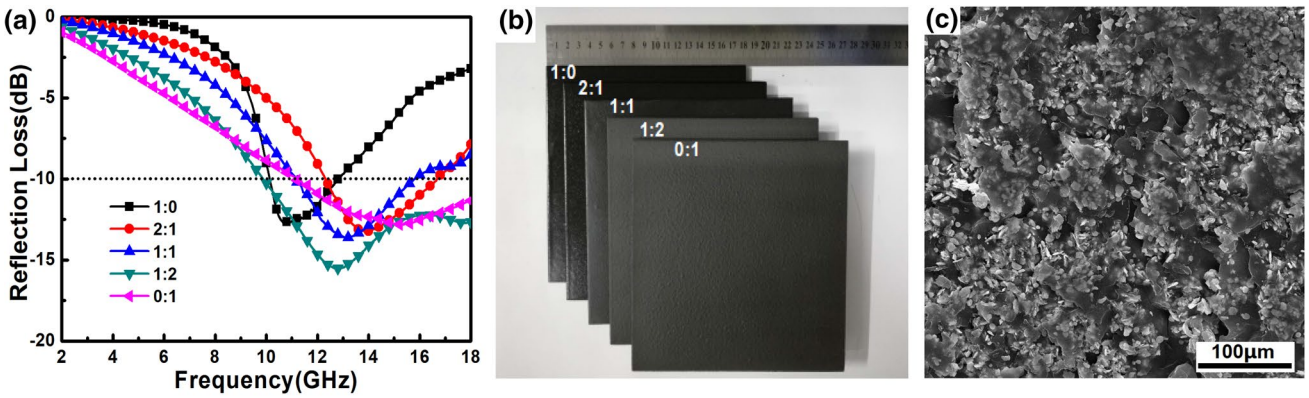

Fig. 5 **a** The measured RL and **b** photograph of absorbing coating based on different mass ratios of Ti_3C_2 MXene/FCI composites; **c** the typical SEM image of coating with mass ratios of 1:2

Table 1 Microwave absorption properties of the FCI-based and Ti_3C_2 MXene-based composites reported recently

Sample	Thickness (mm)	Maximum RL (dB)	f_m (GHz) (maximum RL)	Bandwidth (GHz) (RL < − 10 dB)	Frequency range (GHz)	References
1:0	1.0	− 12.80	10.72	2.80	10.08–12.88	This work
2:1	1.0	− 13.23	13.92	4.48	12.24–16.72	This work
1:1	1.0	− 13.61	13.20	4.72	11.12–15.84	This work
1:2	1.0	− 15.52	12.80	8.16	9.84–18.00	This work
0:1	1.0	− 12.81	15.12	6.88	11.12–18.00	This work
$Ti_3C_2/Ni_{0.5}Zn_{0.5}Fe_2O_4$	6.5	− 42.50	13.50	3.00	12.00–15.00	[13]
Ti_3C_2/Fe_3O_4	1.9	− 57.30	10.10	2.00	9.10–11.10	[14]
Ti_3C_2/CNTs	1.5	− 52.90	4.46	4.46	13.54–18.00	[28]
Ti_3C_2/nano-carbon sphere	2.0	− 19.96	11.90	2.55	10.68–13.24	[29]
FCI/MnO_2	1.5	− 17.78	11.98	8.02	8.84–16.86	[30]
FCI/Ti_3SiC_2	2.4	− 19.20	10.00	3.20	8.47–11.67	[20]

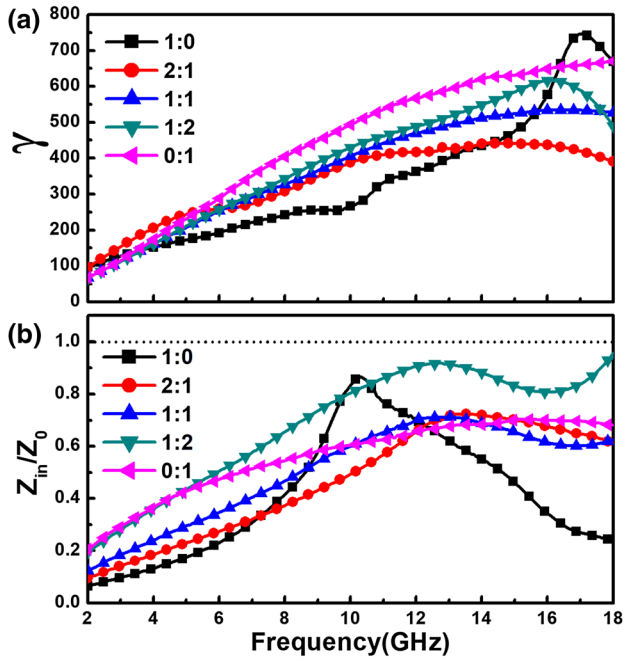

Fig. 6 **a** Attenuation constant versus frequency, and **b** $|Z_{in}/Z_0|$ versus frequency of the Ti_3C_2 MXene/FCI composites with different mass ratios

The γ–f curves of the coating with different mass ratios of Ti_3C_2 MXene/FCI are calculated and displayed in Fig. 6a. The attenuation constant value directly elucidates the amplitude attenuation of electromagnetic waves inside the coating sample. It is unfortunate that the attenuation constant of the coating with mass ratios of 1:2 loading is not the maximum value. According to the Eq. (1), all of the f, ε', ε'', μ' and μ'' value are related to the γ, and larger ε'' and μ" result in higher γ value. Therefore, moderate ε'' and μ'' value for the coating with mass ratios of 1:2 loading presents the middle γ value. However, the absorption performance is also influenced by impedance matching condition. The characteristic impedance $|Z_{in}/Z_0|$ directly decide the EM impedance matching feature, and can be described by the below equation [32]:

$$\frac{Z_{in}}{Z_0} = \sqrt{\frac{\mu_r}{\varepsilon_r}} \tanh\left(j\frac{2\pi fd}{c}\sqrt{\mu_r\varepsilon_r}\right) \quad (2)$$

It is known that if the characteristic impedance $|Z_{in}/Z_0|$ is close to 1, the most of the electromagnetic wave can easily enter into the material, denoting an excellent impedance matching with the free space. According to Eq. (2), we can calculate the normalized input impedance of all samples. As illustrated in Fig. 6(b), the impedance of the coating containing mass ratios of 1:2 is apparently closest to 1 in 2–18 GHz, indicating more electromagnetic wave can enter the coating. This result suggests that combination of the dielectric absorbers and magnetic absorbers possess excellent EM impedance matching feature and considerable EM wave attenuation ability, which finally lead to superior absorbing performance.

4 Conclusion

In summary, the laminated Ti_3C_2 Mxene and flaky carbonyl iron were successfully prepared. The electromagnetic and microwave absorption properties of hybrid Ti_3C_2 MXene/FCI powders were investigated systematically in 2–18 GHz. The electromagnetic parameters and absorbing performance of the hybrid powders could be tuned by simply adjusting the Ti_3C_2 and FCI content. The complex permittivity increased while the complex permeability declined with rising the Ti_3C_2 MXene content. Measured absorbing bandwidth (RL < − 10 dB) of 8.16 GHz is obtained in the coating with 20 wt% Ti_3C_2 MXene and 40 wt% FCI loading and the thickness of 1.0 mm. The Ti_3C_2 MXene/FCI composites with appropriate mass ratio are a promising candidate as broadband microwave absorbent.

Acknowledgements This work was supported by the National Natural Science Foundation of China (Grant No. 61504171).

References

1. Y.R. Wang, Y.P. Pu, Y. Shi, H. Cui, Excellent microwave absorption property of the $CoFe_2O_4/Y_3Fe_5O_{12}$ ferrites based on graphene. J. Mater. Sci. Mater. Electron. **28**, 12866–12872 (2017)
2. B. Zhang, J. Wang, H.Y. Tan, X.G. Su, S.Q. Luo, S. Yang, W. Chen, J.P. Wang, Synthesis of Fe@Ni nanoparticles-modified graphene/epoxy composites with enhanced microwave absorption performance. J. Mater. Sci. Mater. Electron. **29**, 3348–3357 (2018)
3. P.C. Ji, G.Z. Xie, N.Y. Xie, J. Li, J.W. Chen, R.Q. Xu, J. Chen, Fabrication and microwave absorption properties of the flaky carbonyl iron/FeSiAl composite in S-band. J. Mater. Sci. Mater. Electron. **29**, 4711–4716 (2018)
4. Y. Zhang, Y. Huang, T.F. Zhang, C.H. Chang, P.S. Xiao, H.H. Chen, Z.Y. Huang, Y.S. Chen, Broadband and tunable high-performance microwave absorption of an ultralight and highly compressible graphene foam. Adv. Mater. **27**, 2049–2053 (2015)
5. W. Li, T.L. Wu, W. Wang, P.C. Zhai, J.G. Guan, Broadband patterned magnetic microwave absorber. J. Appl. Phys. **116**, 044110 (2014)
6. Q.H. Liu, Q. Cao, H. Bi, C.Y. Lian, K.P. Yuan, W. She, Y.J. Yang, R.C. Chen, $CoNi@SiO_2@TiO_2$ and $CoNi@Air@TiO_2$ microspheres with strong wideband microwave absorption. Adv. Mater. **28**, 486–490 (2015)
7. J. Xiang, X.H. Zhang, Q. Ye, J.L. Li, X.Q. Shen, Synthesis and characterization of FeCo/C hybrid nanofibers with high performance of microwave absorption. Mater. Res. Bull. **60**, 589–595 (2014)
8. H. Wang, Y.Y. Dai, W.J. Gong, D.Y. Geng, S. Ma, D. Li, W. Liu, Z.D. Zhang, Broadband microwave absorption of CoNi@C nanocapsules enhanced by dual dielectric relaxation and multiple magnetic resonances. Appl. Phys. Lett. **102**, 223113 (2013)

9. R.C. Che, L.M. Peng, X.F. Duan, Q. Chen, X.L. Liang, Microwave absorption enhancement and complex permittivity and permeability of Fe encapsulated within carbon nanotubes. Adv. Mater. **16**, 401–405 (2004)
10. M.S. Cao, J. Yang, W.L. Song, D.Q. Zhang, B. Wen, H.B. Jin, Z.L. Hou, J. Yuan, Ferroferric oxide/multiwalled carbon nanotube vs polyaniline/ferroferric oxide/multiwalled carbon nanotube multiheterostructures for highly effective microwave absorption. ACS Appl. Mater. Interfaces **4**, 6949–6956 (2012)
11. Y.C. Qing, W.C. Zhou, F. Luo, D.M. Zhu, Titanium carbide (MXene) nanosheets as promising microwave absorbers. Ceram. Int. **42**, 16412–16416 (2016)
12. W.L. Feng, H. Luo, Y. Wang, S.F. Zeng, L.W. Deng, X.S. Zhou, H.B. Zhang, S.M. Peng, Ti_3C_2 MXene: a promising microwave absorbing material. RSC Adv. **8**, 2398–2403 (2018)
13. Y.B. Li, X.B. Zhou, J. Wang, Q.H. Deng, M. Li, S.Y. Du, Y.H. Han, J.Y. Lee, Q. Huang, Facile preparation of in situ coated $Ti_3C_2T_x/Ni_{0.5}Zn_{0.5}Fe_2O_4$ composites and their electromagnetic performance. RSC Adv. **7**, 24698–24708 (2017)
14. P.J. Liu, Z.J. Yao, V.M.H. Ng, J.T. Zhou, L.B. Kong, K. Yue, Facile synthesis of ultrasmall Fe_3O_4 nanoparticles on MXenes for high microwave absorption performance. Compos. Part A: Appl. Sci. Manuf. **115**, 371–382 (2018)
15. H. Zhao, S.Y. Xu, D.M. Tang, Y. Yang, B.S. Zhang, Thin magnetic coating for low-frequency broadband microwave absorption. J. Appl. Phys. **116**, 243911 (2014)
16. Y.C. Qing, W.C. Zhou, F. Luo, D.M. Zhu, Optimization of electromagnetic matching of carbonyl iron/$BaTiO_3$ composites for microwave absorption. J. Magn. Magn. Mater. **323**, 600–606 (2011)
17. R. Han, L. Qiao, T. Wang, F.S. Li, Microwave complex permeability of planar anisotropy carbonyl-iron particles. J. Alloys Compd. **509**, 2734–2737 (2011)
18. J.H. He, W. Wang, J.G. Guan, Internal strain dependence of complex permeability of ball milled carbonyl iron powders in 2–18 GHz. J. Appl. Phys. **111**, 093924 (2012)
19. O. Khani, M.Z. Shoushtari, K. Ackland, P. Stamenov, The structural, magnetic and microwave properties of spherical and flake shaped carbonyl iron particles as thin multilayer microwave absorbers. J. Magn. Magn. Mater. **428**, 28–35 (2017)
20. Y. Liu, X.L. Su, F. Luo, J. Xu, J.B. Wang, X.H. He, Y.H. Qu, Enhanced electromagnetic and microwave absorption properties of carbonyl iron/Ti_3SiC_2/epoxy resin coating. J. Mater. Sci. Mater. Electron. **29**, 2500–2508 (2018)
21. J. He, H. Luo, L.H. He, S.Q. Yan, D.Y. Shan, S.X. Huang, L.W. Deng, Investigation on microwave dielectric behavior of flaky carbonyl iron composites. J. Mater. Sci. Mater. Electron. **29**, 15112–15118 (2018)
22. J. He, L.W. Deng, H. Luo, L.H. He, D.Y. Shan, S.Q. Yan, S.X. Huang, Electromagnetic matching and microwave absorption abilities of Ti_3SiC_2 encapsulated with $Ni_{0.5}Zn_{0.5}Fe_2O_4$ shell. J. Magn. Magn. Mater. **473**, 184–189 (2019)
23. D. Micheli, C. Apollo, R. Pastore, P. Roberto, B.M. Ramon, L. Susanna, M. Mario, Nanostructured composite materials for electromagnetic interference shielding applications. Acta Astronaut. **69**, 747–757 (2015)
24. H.M. Tahir Farid, I. Ahmad, I. Ali, A. Mahmood, S.M. Ramay, Structural and dielectric properties of copper-based spinel ferrites. Eur. Phys. J. Plus **133**, 41–53 (2018)
25. K. Bibi, I. Ali, M. Tahir Farid, A. Mahmood, S.M. Ramay, K. Ali, Electric and dielectric properties of ytterbium substituted spinel ferrites. J. Mater. Sci. Mater. Electron. **29**, 3744–3750 (2018)
26. H.M. Tahir Farid, I. Ahmad, I. Ali, S.M. Ramay, A. Mahmood, G. Murtaza, Dielectric and impedance study of praseodymium substituted Mg-based spinel ferrites. J. Magn. Magn. Mater. **434**, 143–150 (2017)
27. M. Tahir Farid, I. Ahmad, M. Kanwal, I. Ali, Effect of praseodymium ions on manganese based spinel ferrites. Chin. J. Phys. **55**, 813–824 (2017)
28. X.L. Li, X.W. Yin, M.K. Han, C.Q. Song, H.L. Xu, Z.X. Hou, L.T. Zhang, L.F. Cheng, Ti_3C_2 MXenes modified with in situ grown carbon nanotubes for enhanced electromagnetic wave absorption properties. J. Mater. Chem. C **5**, 4068–4074 (2017)
29. B.Z. Dai, B. Zhao, X. Xie, T.T. Su, B.B. Fan, R. Zhang, R. Yang, Novel two-dimensional $Ti_3C_2T_x$ MXenes/nano-carbon sphere hybrids for high-performance microwave absorption. J. Mater. Chem. C **6**, 5690–5697 (2018)
30. W.Q. Zhang, S.W. Bie, H.C. Chen, Y. Lu, J.J. Jiang, Electromagnetic and microwave absorption properties of carbonyl iron/MnO_2 composite. J. Magn. Magn. Mater. **359**, 1–4 (2014)
31. J. Zhang, L.X. Wang, Q.T. Zhang, Electromagnetic properties and microwave-absorption properties of $BaTiO_3/BaZn_2Fe_{16}O_{27}$ composite in 2–18 GHz. J. Mater. Sci. Mater. Electron. **25**, 5601–5605 (2014)
32. J. He, L.W. Deng, S. Liu, S.Q. Yan, H. Luo, Y.H. Li, L.H. He, S.X. Huang, Enhanced microwave absorption properties of Fe_3O_4-modified flaky FeSiAl. J. Magn. Magn. Mater. **444**, 49–53 (2017)